Journal of Membrane Science 331 (2009) 57–65

Contents lists available at ScienceDirect

Journal of Membrane Science

journal homepage: www.elsevier.com/locate/memsci

NaA zeolite as an effective diffusion barrier in composite Pd/PSS membranes

M.L. Bosko, F.Ojeda, E.A. Lombardo, L.M. Cornaglia*

Instituto de Investigaciones en Catálisis y Petroquímica (FIQ, UNL-CONICET), Santiago del Estero 2829, 3000 Santa Fe, Argentina

ARTICLE INFO

Article history:
Received 15 November 2008
Received in revised form 30 December 2008
Accepted 6 January 2009
Available online 14 January 2009

Keywords:
Hydrogen purification
Zeolite synthesis
Pd membrane

ABSTRACT

Palladium composite membranes on porous stainless steel were prepared by electroless plating. In order to obtain a thin palladium film, an intermediate layer was necessary to modify the pore size of the substrate and form a diffusion barrier between the palladium film and the support. The NaA zeolite, used as intermediate, was synthesized by vacuum-assisted secondary growth. Pure gas permeability tests were conducted using hydrogen and nitrogen between 400 and 450 °C. The surface morphology and the components of the different layers of the membrane were characterized by scanning electron microscopy (SEM), energy-dispersive X-ray analysis (EDS), X-ray photoelectron spectroscopy (XPS), and X-ray diffraction (XRD). When vacuum was applied during the zeolite synthesis at 80 °C, the Pd membrane showed high H_2/N_2 ideal selectivity in the working temperature range. This result suggests that NaA zeolite is an effective intermediate substrate modifier when an appropriate synthesis method is employed.

1. Introduction

Hydrogen separation technologies are of great importance due to the essential nature of hydrogen as an alternative, clean, energy-efficient carrier and to the increasing demand for hydrogen in various chemical and petrochemical industries. Membrane-related processes are considered to be one of the most promising routes for the production of high purity hydrogen, which is necessary for semiconductor and fuel cell applications. Dense Pd membranes are attractive due to their perfect perm-selectivity to hydrogen; however, their thicknesses of at least ca. 50 μm limit their use because of their low permeance and high cost. Thin Pd-based films supported on porous substrates constitute an economic option to overcome these limitations.

Porous ceramic materials, glass and stainless steel were successfully used as supports for palladium membranes. Ceramic supports have robustness, chemical stability and superior upper temperature limit. It has been reported that porous ceramic supports with rougher surfaces and larger pores favor the adhesion of the palladium films [1]. Furthermore, porous stainless steel (PSS) are promising substrates due to their good mechanical strength, more resistance to cracking, operation at high pressures and simplicity of module construction [2]. Composite Pd/PSS membranes, welded on both ends to non-porous stainless steel tubes, can be easily assembled and integrated into an associated process.

Nevertheless, the big pores and roughness of the PSS surface impair the preparation of a thin defect-free Pd membrane on porous stainless steel substrates. Therefore, it is convenient to modify both the pore size of the substrate and its surface roughness with an intermediate component [3]. The penetration of this material in the pore system of the substrate is a rational strategy to prepare a more compact structure. Thus, when the material is submitted to large temperature changes, the thermal expansion between both components will have lesser effects. This intermediate is also expected to be a diffusion barrier to inhibit the migration of the substrate components to the Pd layer [2,4], which will deteriorate the performance of the composite membrane. Su et al. [3] reported thin palladium membranes selective to hydrogen, with a thin SiO_2 coating in order to modify the pore size of the PSS, decrease the surface roughness, and act as diffusion barrier. A different alternative was applied by Tong et al. [5]. They employed asymmetric porous stainless steel (APSS) with a relative smooth top layer consisting of stainless steel fibers (micrometer size) as support, obtaining stable membranes with high fluxes. Oxide materials such as Fe_2O_3 generated by in situ oxidation [6–8], Al_2O_3 [7], colloidal silica [3,9], TiO_2 [4] and ZrO_2 [4,10] were applied on the porous substrates. Zeolites are particularly appropriate for this application since they present several advantages such as high thermal resistance, chemical inertness, and high mechanical strength [11].

In recent years, zeolites have been employed as membrane materials. The MFI-type zeolite membranes have shown good results in the separation of organic molecules because the MFI zeolite has a channel opening size close to the cross-section of key raw materials, e.g., butane and xylene isomers [12]. The A-type zeolite membrane has been proposed for the separation of several industrially important gases. Its pore diameter is similar to the cross-section of molecules such as H_2 and N_2; therefore, it is expected to be effective in the separation of these gases from short-

* Corresponding author at: Tel.: +54 342 4536861; fax: +54 342 4571162.
E-mail address: lmcornag@fiq.unl.edu.ar (L.M. Cornaglia).

0376-7388/$ – see front matter © 2009 Elsevier B.V. All rights reserved.
doi:10.1016/j.memsci.2009.01.005

chain alkanes [11]. Miachon et al. [13] synthesized a nanocomposite MFI-alumina membrane via pore-plugging. By optimizing the synthesis conditions, an average increase of one order of magnitude in the separative performance was obtained. Recently, Huang et al. [14] reported the preparation of a NaA zeolite membrane on a tubular α-Al_2O_3 support with a vacuum-assisted method. This membrane showed a good pervaporation performance, with a separation factor (water/isopropanol) close to 3800.

The goal of the present work was to prepare palladium membranes on a porous support using the NaA zeolite as intermediate due to its simple synthesis, thermal resistance and low cost. The zeolite was obtained by in situ hydrothermal synthesis onto a PSS by the vacuum-assisted secondary growth method to favor the penetration of the zeolite crystals into the pores of the substrate. The palladium film was deposited by electroless plating. The membranes were characterized by SEM, EDS, XPS, XRD, and permeation measurements.

2. Experimental

2.1. Stainless steel support

Composite palladium-PSS membranes were prepared using the electroless deposition method. 0.2 μm grade PSS supports were purchased from Mott Metallurgical Corporation, with 6.4 mm i.d. and 9.5 mm o.d. The grade of the support was determined by the manufacturer guaranteeing a 99.9% rejection of 0.2 μm spherical particles by the interconnected porosity. Prior to deposition, one end of the PSS was welded to a non-porous stainless steel tube and the other one to a non-porous SS plug. The supports were cleaned in ultrasonic bath with acetone for 1 h to remove organic contaminants and dirt, and then dried overnight at 80 °C.

2.2. Synthesis of NaA zeolite

The method employed was secondary growth synthesis [11,14]. The seeding layer was coated on the outer surface of the support by the vacuum-assisted seeding method using an ejector water jet pump, which was used to generate a pressure difference between the two sides of the support walls. The tube connected to a vacuum system was fixed vertically and twice immersed for 1 min in a cylindrical vessel containing a colloidal suspension. This suspension was prepared by dispersing 2 g of A-type zeolite seed in 10 ml of water in an ultrasonic bath, followed by a centrifugation step to obtain the final suspension.

In order to prepare the synthesis gel, two precursor solutions (aluminate and silicate) were mixed with vigorous stirring at the synthesis temperature. The aluminate solution was prepared by dissolving 7.70 g of sodium hydroxide and 6.07 g of sodium aluminate in 120 ml deionized water at room temperature. The silicate solution was prepared by mixing 3.56 g of silica and 53.3 ml of deionized water [15].

The seeded support was placed vertically in a container with the synthesis gel. In some cases, vacuum was applied using the system shown in Fig. 1. The inner and outer part of the support were washed with deionized water, and then dried at 80 °C overnight. The zeolite A membranes were synthesized at either 80 °C for 8 h or 90 °C for 3 h. The modified supports were calcined in air at 400 and/or 550 °C during 1 h. Two or three hydrothermal syntheses were performed until the N_2 permeance was within the 10^{-9} mol^{-2} m^{-2} s^{-1} Pa^{-1} range.

2.3. Metallic deposition

The modified substrates were activated by conventional $SnCl_2$/$PdCl_2$ activation procedure [16]. The solution concentrations

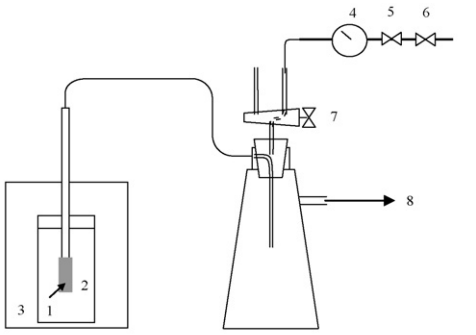

(1) Support
(2) Seed suspension or synthesis gel
(3) Thermal bath
(4) Manometer
(5) Needle valve
(6) On-off valve
(7) Three-way valve
(8) Ejector water jet pump

Fig. 1. System for zeolite synthesis.

were 1.13 g/l of $SnCl_2 \cdot 2H_2O$ (pH 2) and 0.88 g/l of $PdCl_2$ (pH 2). Electroless plating (ELP) was used to coat the PSS composite with a continuous palladium layer. The plating bath contained a solution of $PdCl_2$ (3.6 g/l), HCl (37%, 5 ml/l), NH_4OH (28%, 650 ml/l), $Na_2EDTA \cdot 2H_2O$ (67 g/l) and N_2H_4 (1 M, 10 ml/l). This composition was similar to the one reported by Yeung et al. [17]. The nonporous stainless steel parts were covered with Teflon, and then the modified substrates were immersed in the plating bath for 90 min several times. The deposition temperature was maintained at 50 °C throughout the preparation. The as-deposited membrane was carefully rinsed with deionized water between each plating step, and the plating bath was renewed. When the plating was finished, the membrane was rinsed with water and finally dried at 120 °C overnight and weighed. This procedure was repeated until the membrane was dense. The gas-tightness in each membrane was examined using nitrogen gas at a pressure of 10–20 kPa at room temperature. The thickness was estimated from the weight gain after palladium plating and checked by SEM. The membranes were heated in a nitrogen flow and the heating rate was 0.5 °C/min. Before the first measurement of hydrogen permeability, the membranes were activated in a hydrogen flow for 6 h at 400 °C.

2.4. X-ray diffraction

The XRD patterns of the films were obtained with an XD-D1 Shimadzu instrument, using Cu Kα radiation at 30 kV and 40 mA. The scan rate was 1–2° min^{-1} in the range 2θ = 15–90°.

2.5. Scanning electron microscopy, energy-dispersive X-ray analysis

The outer surface and cross-section images were obtained using a JEOL scanning electron microscope, model JSM-35 C, equipped with an energy dispersive analytical system (EDAX). For the cross-section views, tubular pieces with a length of ~12 mm were placed in a plastic tube; then epoxy resin was added. After hardening, they were cut. The grinding was carried out with waterproof abrasive paper of 180, 280, 500, 800 and 1200 grit. The polishing was done with a ~1-μm-grade paste, and finally with a suspension of γ-alumine (50 nm). The grinding and the polishing cycles lasted 5 min; after each cycle, it was necessary to clean the samples with ethyl alcohol in ultrasonic bath.

2.6. X-ray photoelectron spectroscopy

XPS analyses were performed in a multi-technique system (SPECS) equipped with a dual Mg/Al X-ray source and a hemi-

spherical PHOIBOS 150 analyzer operating in the fixed analyzer transmission (FAT) mode. The spectra were obtained with a pass energy of 30 eV; the Mg Kα X-ray source was operated at 100 W and 10 kV. The working pressure in the analyzing chamber was less than 5×10^{-10} kPa. The XPS analyses were performed on the modified support and on the used Pd-membranes after being exposed to ambient conditions. The Pd membranes were heated up in flowing H_2/Ar at 425 °C, and the zeolite modified substrates were heated up in vacuum at the same temperature in the reaction chamber of the spectrometer. The spectral Pd 3d, Pd 3p, O 1s, C 1s, Si 2p, Na 1s, Fe 2p and Al 2p were recorded for each sample. The data treatment was performed with the Casa XPS program (Casa Software Ltd., UK). The peak areas were determined by integration employing a Shirley-type background. Peaks were considered to be a mixture of Gaussian and Lorentzian functions in a 70/30 ratio. For the quantification of the elements, sensitivity factors provided by the manufacturer were used.

2.7. Gas permeation measurements

Thermal treatments and gas permeation measurements were conducted in a shell-and-tube membrane module. The open end of the membrane was sealed to the permeator wall with Teflon ferrules. The permeator was placed in an electrical furnace and heated to the desired temperatures. A thermocouple within the membrane tube monitored and controlled the temperature during the experiments. All the gases were fed to the permeator using calibrated mass-flow controllers. Feed gases flowed along the outside of the membrane while the permeated gases flow rates were measured in the inner side of the membrane. A N_2 sweep gas stream was fed in the permeate side only during the heating and cooling periods. Pressure differences across the membranes were controlled using a back-pressure regulator. The upstream was varied while keeping the downstream pressure constant at 100 kPa. The gas permeation flow rates of either H_2 or N_2 were measured using two bubble flow meters at room temperature and pressure. All the membranes were tested over a period of more than 100 h.

3. Results and discussion

3.1. Modified support

The support was modified with NaA zeolite by hydrothermal synthesis with secondary growth, employing different temperatures, times and vacuum conditions (Table 1). The NaAZ90-vac/PSS and the NaAZ80-vac/PSS were synthesized with vacuum assistance during the hydrothermal synthesis, while the NaAZ80/PSS was obtained without vacuum.

Fig. 2 shows the XRD pattern of the powder collected after the hydrothermal synthesis of NaAZ90-vac/PSS at 90 °C. The diffractogram reveals that a highly crystalline NaA zeolite [18] was obtained. The strongest peaks are seen at 34°, 29.8°, 27°, 23.9° and 21.6°. The same reflections, with lower intensities, are observed in the XRD profile of the modified substrate after oxidation at 400 °C (Fig. 3). Besides, two peaks at 43.6° and 50.7° pertaining to the support can be observed, assigned to the γ-phase (austenite) [2,19]. The other modified supports after the zeolite hydrothermal synthesis at 80 °C show similar XRD patterns.

Table 1
Hydrothermal synthesis conditions of the NaA zeolite.

PSS modified	Synthesis temperature (°C)	Vacuum	Time (h)	ΔM (%)
NaAZ90-vac/PSS	90	Yes	3	0.084
NaAZ80/PSS	80	No	8	0.244
NaAZ80-vac/PSS	80	Yes	8	0.211

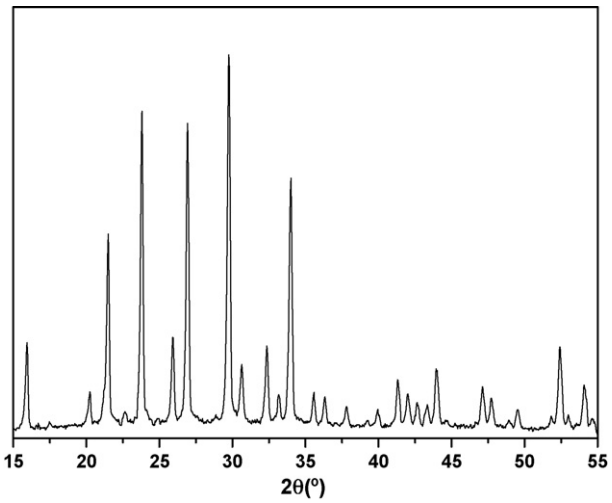

Fig. 2. XRD pattern of NaA zeolite powder collected after the synthesis of NaAZ90-vac/PSS.

The surface and cross-sectional morphological characteristics of the modified supports were examined by SEM. The top view forNaAZ90-vac/PSS (Fig. 4A) shows typical aggregates of cubic NaA zeolite crystals and their uniform distribution on the support [20]. The size of zeolite crystals was between 2 and 10 μm. There is an important intergrowth among the aggregates. The cross-section view (Fig. 4B of NaAZ90-vac/PSS) shows zeolite crystals located in the pore openings of the support.

The top view of NaAZ80/PSS (Fig. 4A) shows well-intergrown zeolite crystals but of a smaller size (1–3 μm). The top view SEM image of NaAZ80-vac/PSS (Fig. 4A) shows a uniform distribution of cubic NaA zeolite crystals on the support, but an incomplete intergrowth among these aggregates. Some edges and corners of individual crystals as well as ridges between crystal aggregates are evident. In this layer, a narrower crystal size distribution is observed compared with that of previous substrates. Besides, the average size was ~1.5–2 μm, smaller than the previous ones. The cross-section view (Fig. 4B of NaAZ80-vac/PSS) shows a homogeneous deposition of the zeolite.

The cross-section views of all the modified supports show the penetration of the zeolite crystals into the pore system. This can be

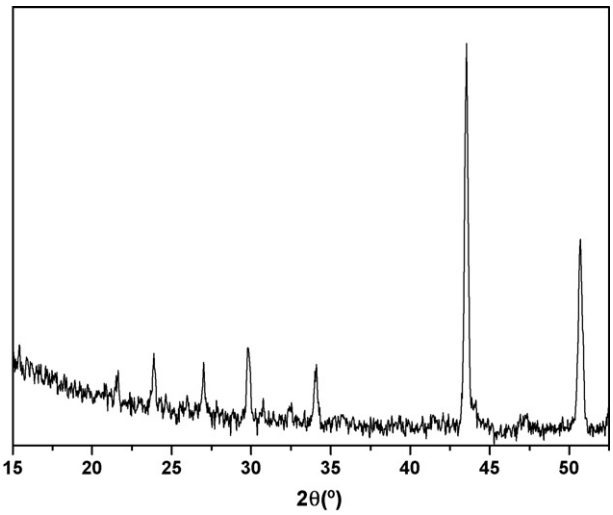

Fig. 3. XRD pattern of the NaA zeolite synthesized on the seeded porous support at 90 °C, total synthesis time of 6 h (two-stage) with vacuum assistance and subsequent calcination at 400 °C.

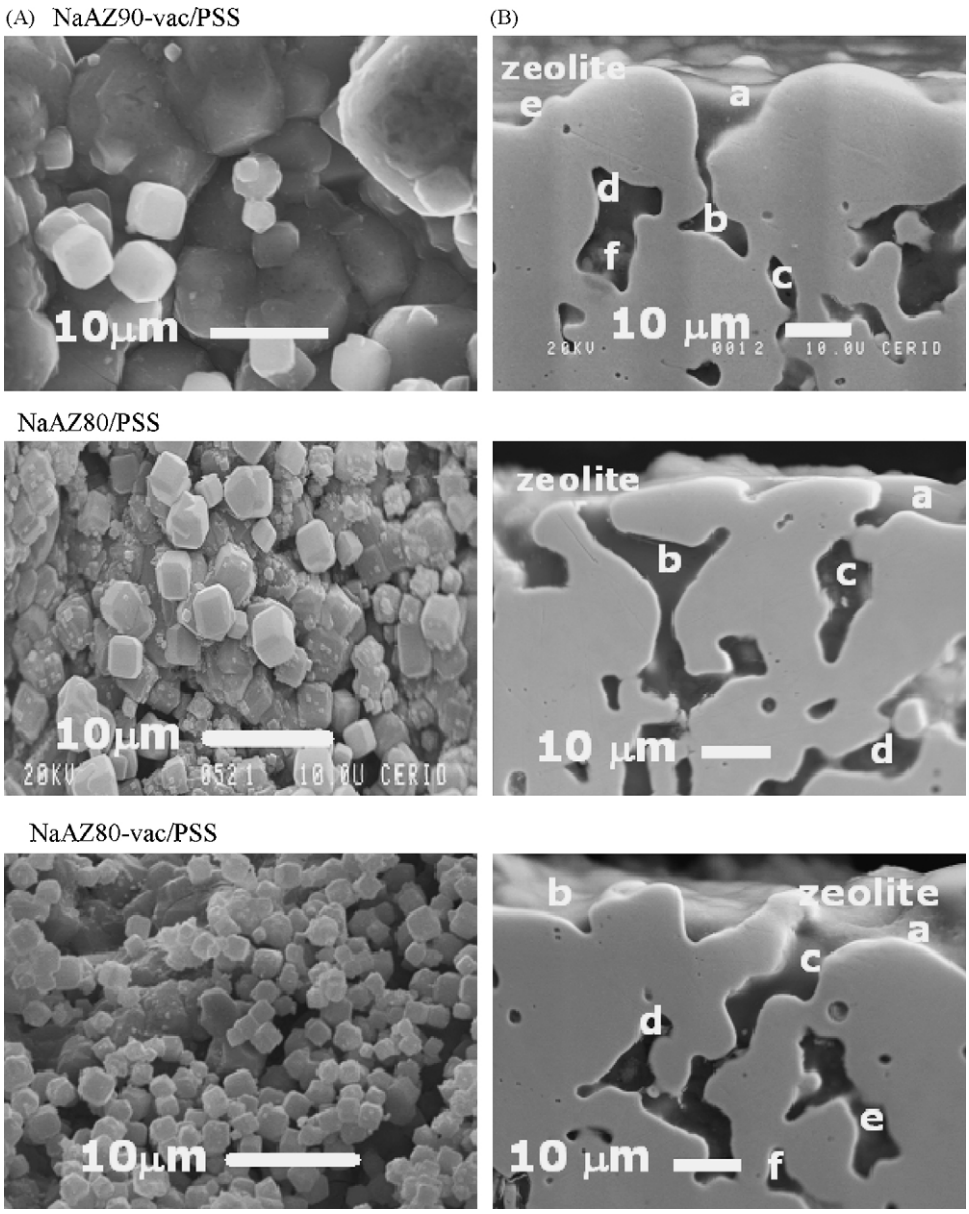

Fig. 4. SEM images of (A) top view of the NaA crystals and (B) cross-section view of the modified supports.

attributed to the vacuum seeding. According to Huang et al. [21] in the vacuum process the zeolite seeds migrate to the support surface under the common action of the gravitation, capillary and vacuum forces. The colloidal suspension is sucked into the support pores by the differential pressure. Therefore, the zeolite seeds are attracted and transported onto the support surface continuously. In this process, the negative influence of the gravitation force can be offset to a certain extent by applying vacuum. The zeolite seeds could thus form a much smoother, uniform and compact seeding layer.

The elemental chemical analysis was performed both at the bulk and surface level. The volumetric EDS data that were taken at the a–f locations (Fig. 4B) are collected in Table 2. On the cross-section views (Fig. 4B), the growth of the NaA zeolite inside the pores can be observed in agreement with EDS results. At points a–f (see Table 2) both Si and Al were measured, and the average ratio was close to the A-zeolite bulk value (Si/Al = 1). The Fe/Al ratio measured at the pore mouth (point a) presented low-values of ~0.03.

The XPS data (Table 3) show a surface Si/Al atomic ratio lower than 1 for the NaAZ80-vac/PSS and NaAZ80/PSS samples. This result suggests an aluminum enrichment of the zeolite surface. Note that neither Fe nor Ni are present on the modified support surface of NaAZ90-vac/PSS and NaAZ80/PSS. However, low concentrations of Fe and Ni were detected in the NaAZ80-vac/PSS sample. These

Table 2
Relative concentrations measured on the sample cross-section for modified supports and membranes.

Sample	Fe/Al[a]	Si/Al[b]	Pd/Fe[b]	Fe[a] (%)
NaAZ90-vac/PSS	0.030	1.14	–	1
NaAZ80/PSS	0.028	1.18	–	1
NaAZ80-vac/PSS	0.028	1.11	–	1
Pd/NaAZ90-vac/PSS	nd[c]	0.89	nd[c]	nd[c]
Pd/NaAZ80/PSS	0.38	0.94	27.7	3
Pd/NaAZ80-vac/PSS	nd[d]	1.00	99	1

[a] Measured at point "a" shown in the SEM image.
[b] Average Si/Al ratio calculated from EDS data of the SEM image points (a–f) (see Figs. 4 and 7).
[c] No Fe detected.
[d] No Al detected.

Table 3
Relative surface concentrations on modified supports determined by XPS.

PSS modified	Si/Al	Na/Al	Fe/Al	Ni/Al
NaAZ90-vac/PSS	1.02	0.92	nd[a]	nd[a]
NaAZ80/PSS	0.3	1.6	nd[a]	nd[a]
NaAZ80-vac/PSS	0.67	1.03	0.11	0.13

[a] Neither Fe or Ni detected.

results can be attributed to the formation of a continuous thin layer on the support, particularly for the NaAZ80/PSS and NaAZ90-vac/PSS composites.

To check the effectiveness of the zeolite deposit, permeation measurements were performed on the three modified supports (Table 4). The lowest nitrogen permeability was observed on the NaAZ90-vac/PSS (3×10^{-8} mol m^{-2} s^{-1} Pa^{-1}) modified support. This support also showed the lowest percentage mass change after the NaA synthesis (0.084%) (see Table 1). This can be attributed to the larger size of crystals that impairs the access into the porous structure (Fig. 4A). This support was calcined at 400 °C only.

The modified support, prepared without vacuum, shows nitrogen permeances of 7.3 and 5.2×10^{-7} mol m^{-2} s^{-1} Pa^{-1} after oxidation at 400 and 550 °C, respectively. For both membranes synthesized at 80 °C, the weight increases with the number of synthesis and calcinations, and the percentage change in mass was ca. 0.20% (Table 1). The NaAZ80-vac/PSS shows a nitrogen permeance of 2.5×10^{-7} mol m^{-2} s^{-1} Pa^{-1} after the hydrothermal synthesis and subsequent oxidation.

The NaA zeolite has been previously synthesized for H_2 separation from short-chain alkanes and pervaporation processes. Tiscareño-Lechuga et al. [15] prepared NaA membranes under a centrifugal force field in order to promote the formation of denser, more continuous layers. The synthesis temperature was 100 °C and tubular alumina (200–1000 nm) was employed as support. The highest He/N_2 ideal perm-selectivity and best permeance were obtained in a membrane with a thickness of 7–10 μm; the values were 3.8 and 4.4×10^{-7} mol m^{-2} s^{-1} Pa^{-1}, respectively. The selectivity value was slightly higher than the corresponding Knudsen ideal perm-selectivity (2.65).

Xu et al. [18] obtained high quality membranes by employing the multi-step synthesis at 90 °C. The best NaA zeolite membrane was obtained with a three-step synthesis on an α-Al_2O_3 support. The membrane thickness was 16 μm. The N_2 permeance was 1.2×10^{-8} mol m^{-2} s^{-1} Pa^{-1} and the O_2/N_2 selectivity was 2.61, slightly above that of the Knudsen transport (0.94).

Huang et al. [14,21] synthesized NaA membranes with the vacuum-assisted method in order to reduce the negative influence of the gravitation force. They obtained uniform, dense membranes whose properties were evaluated by pervaporation for dehydration of 95% isopropanol/water mixtures. They did not report N_2 permeances.

In our case, the N_2 permeances were in the same range as those reported above but ultra-thin layers were obtained (see Fig. 4B). It can be seen that the NaA zeolite penetrates into the pore system but there is no well-defined zeolite layer on top of the substrate surface.

3.2. Pd membranes

Electroless plating is an autocatalytic reaction. The Pd deposition was performed after the conventional activation with $SnCl_2$ and $PdCl_2$ solutions to produce a uniform coverage of the surface with small palladium seeds.

The X-ray diffraction patterns (not shown) after the Pd depositions on the modified supports only display the reflection peaks of pure palladium (40.1°, 46.7°, 68.1° and 82.1°) [22]. No peaks from the modified PSS support were observed.

SEM micrographs of the Pd/NaAZ90-vac/PSS membrane after the permeation measurements (Fig. 5) show the largest palladium grain size (20–40 μm) and the grain boundaries are very notorious. The palladium thickness was 22–27 μm (Fig. 6). In this membrane, the Pd penetrated quite deep into the pore system and the resulting Pd layer exhibited thicknesses that were at some points (inside the pores) larger than the ones calculated by the gravimetric technique.

Table 2 shows the Fe content in the Pd-zeolite interphase region (point a) (Fig. 6B). In the case of the Pd/NaAZ90-vac/PSS sample, Fe is not present at this interphase; however, a low percentage of Fe was detected for both the Pd/NaAZ80/PSS and Pd/NaAZ80-vac/PSS membranes. Note that the working temperatures were between 400 and 450 °C and that the permeation measurements were performed during 250 h.

The Pd 3d, Pd 3p and O 1s spectra of palladium membranes after the permeation measurements at high temperature are shown in Fig. 7. The O 1s peak overlaps the Pd $3p_{1/2}$ and Pd $3p_{3/2}$ signals. In all the used membranes after exposure to ambient conditions, the oxygen peak was the main detected peak in this region. However, the Pd $3d_{5/2}$ binding energy was 335.4 ± 0.1 eV for the used membranes without in situ treatment (Fig. 7A). This value corresponds to pure Pd [23], suggesting that Pd was not oxidized when the membranes were exposed to ambient conditions. When the membranes were treated with a hydrogen flow at 400 °C in the load lock spectrometer chamber, the O 1s peak disappeared and the Pd $3p_{1/2}$ and Pd $3p_{3/2}$ peaks became well-resolved with a $3p_{1/2}/3p_{3/2}$ intensity ratio close to the expected value of 0.5 (see Fig. 7B). Besides, the Pd $3d_{5/2}$ binding energy was not modified.

3.3. Permeation measurements

The permeation measurements were carried out at 400 and 450 °C, the permeate side was maintained at atmospheric pressure, and the pressure difference applied was varied from 10 to 120 kPa. Fig. 8 shows the hydrogen fluxes vs $\Delta P^{0.5}$. The Pd/NaAZ80-vac/PSS membrane shows the highest values for the hydrogen flux, in the measured pressure range at 450 °C. Note that the hydrogen flux increases linearly with $\Delta P^{0.5}$ at the two temperatures studied. This trend is consistent with the solution-diffusion mechanism of pure hydrogen through a palladium membrane, when the rate-determining step is the diffusion of H in the metallic film. Under

Table 4
N_2 permeance trough the modified supports[a].

PSS modified	N_2 permeance (mol m^{-2} s^{-1} Pa^{-1})				
	1st synthesis	2nd synthesis	3rd synthesis	Oxidation (400 °C)	Oxidation (550 °C)
NaAZ90-vac/PSS	Not tested	2×10^{-6}	Dense	3×10^{-8}	–
NaAZ80/PSS	1.8×10^{-5}[b]	9.1×10^{-6}	Dense	7.3×10^{-7}	5.2×10^{-7}
NaAZ80-vac/PSS	1.3×10^{-5}	5.4×10^{-9}[c]	–	–	2.5×10^{-7}

[a] T = 25 °C, ΔP = 50 kPa.
[b] Measured at 20 kPa.
[c] Measured at 100 kPa.

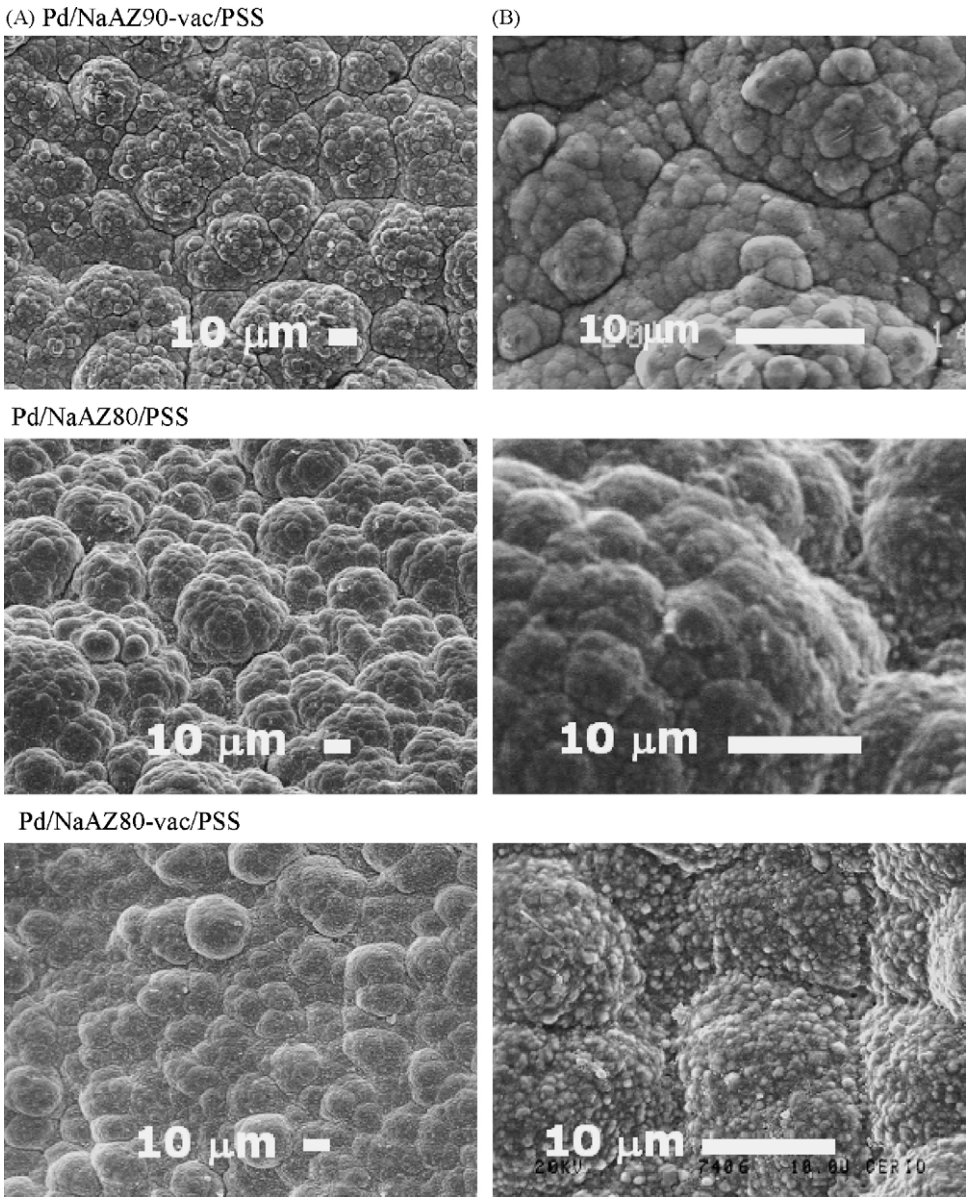

Fig. 5. SEM micrographs (top view) of the palladium membranes, with different magnifications after the permeation measurements.

such conditions, the hydrogen flux can be expressed by Sievert's law:

$$J = \frac{Q_0}{L} \exp\left[-\frac{E_p}{RT}\right] (P_{H_2\,ret}^{0.5} - P_{H_2\,per}^{0.5})$$

where J is the hydrogen flux (mol m^{-2} s^{-1}), L the membrane thickness (m), Q_0 the pre-exponential factor (mol m^{-1} s^{-1} Pa$^{-0.5}$), E_p the activation energy of permeability (J mol^{-1}), $P_{H_2\,ret}$ and $P_{H_2\,per}$ the partial hydrogen pressures in the retentate and permeate, respectively, T (K), and R the gas constant (8.314 J mol^{-1} K^{-1}).

This expression shows that an increase in the hydrogen flux can be achieved by decreasing the thickness of the palladium layer. In our membranes, the thicknesses decrease in the following order: L (Pd/NaAZ90-vac/PSS) > L (Pd/NaAZ80/PSS) > L (Pd/NaAZ80-vac/PSS), and the hydrogen fluxes increase in the same order. These results show that the dependence of the hydrogen flux follows Sievert's law.

Fig. 9 shows the ideal selectivity, defined as the ratio of the fluxes of two pure gases (H_2 and N_2), under the same trans-membrane pressure difference and temperature. In the three synthesized membranes, the ideal selectivities decrease with increasing pressure difference and when the temperature is decreased. This behavior can be explained by taking into account the possible permeation mechanisms. The hydrogen permeates mainly through the solution-diffusion mechanism in the palladium film; this flux is proportional to $\Delta P^{0.5}$ and increases with temperature. On the other hand, the nitrogen flux is governed by Knudsen diffusion (mesopores) and viscous flux (macropores). The dependence of the latter two mechanisms with ΔP is linear and both fluxes decrease with temperature. Therefore, one could expect that selectivities increase with temperature. However, in all our membranes only a slight selectivity increase was observed, probably due to the pinhole formation during the temperature cycling performed in the long-term operation. Note that the Pd/NaAZ80-vac/PSS and Pd/NaAZ80/PSS membranes were tested during more than 250 h.

The best performance was observed for the Pd/NaAZ80-vac/PSS membrane, whose hydrogen permeance and selectivity were 1.12×10^{-3} mol m^{-2} s^{-1} Pa$^{-0.5}$ and 608, at 450 °C and 50 kPa (Table 5). These results suggest that the zeolite synthesis at 80 °C

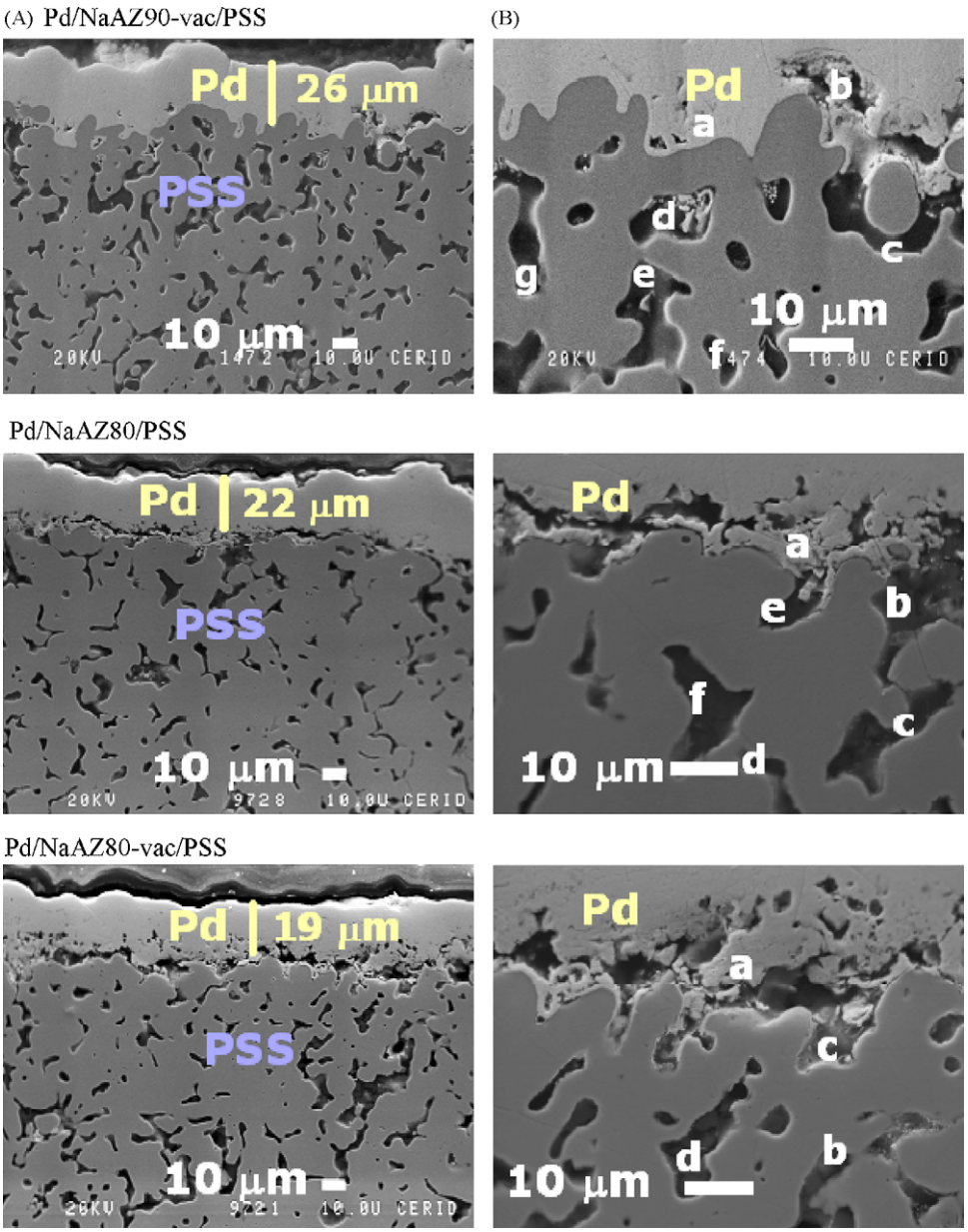

Fig. 6. Cross-section views of palladium membranes with different magnifications after the permeation measurements.

with vacuum yields an effective modifier. The possible explanation is that the small crystals obtained can easily enter the porous system which causes less membrane defects. Morón et al. [24] modified the NaA membranes by either CVD of a Pd compound or impregnation with a Pd salt solution in order to minimize the non-selective defects by Pd deposition. They sustained that a modest improvement was obtained with a H_2/N_2 ideal selectivity equal to 3.98, barely above the theoretical Knudsen value (3.74).

Ceramic Pd composite membranes and self-supported Pd membranes were developed with high selectivity and permeation fluxes. Bredesen and co-workers [25] developed thin, self-supported, defect-free Pd/23% Ag membranes (1.6 μm). The membranes were 100% selective to hydrogen employing a constant differential pressure of 3 kPa throughout the permeation measurements. After 100 days of operation the H_2/N_2 perm-selectivity still laid around 500.

Table 5
Hydrogen fluxes and ideal selectivities of thin palladium membranes.

Membrane	Support[a]	Diffusion barrier	Pd (μm)	T (°C)	ΔP (kPa)	H_2 flux (mol m^{-2} s^{-1})	Permeance (mol m^{-2} s^{-1} Pa$^{-0.5}$)	H_2/N_2 selectivity
Pd/NaAZ80-vac/PSS	316L (0.2)	NaAZ	19	450	50	0.0790	1.1×10^{-3}	608
Rothenberger et al. [27]	316L (0.2)	Fe_2O_3	22	450	101	0.0853	2.7×10^{-4}	∞[b]
Su et al. [3]	316L (0.2)	SiO_2	6	500	50	0.133	1.9×10^{-3}	450
Huang et al. [8]	310L (0.5)	ZrO_2	23	400	110	0.0734	5.2×10^{-4}	320

[a] Support grades(in μm) are given between parentheses.
[b] Valid when the membrane was subject to a pressure differential below 138 kPa.

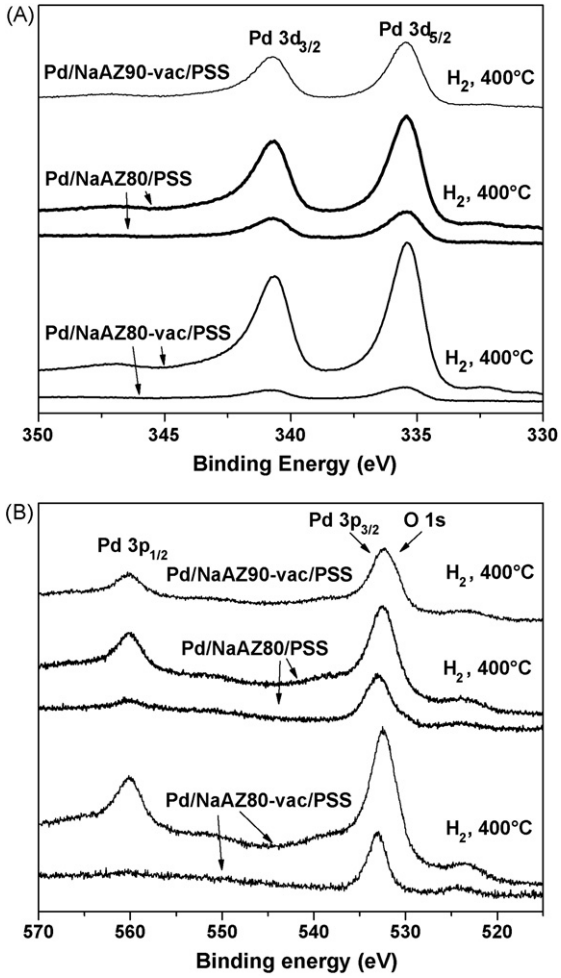

Fig. 7. XP spectra of Pd 3d (A) and Pd 3p–O 1s (B) for the palladium membranes after hydrogen permeation measurements at high temperatures: exposed to ambient conditions and after in situ reduction at 400 °C.

Ceramic supports were employed to synthesize Pd–Cu membranes by electroless plating with high hydrogen selectivities such as 1400 at 500 °C and 344.7 kPa [26]. Structural factors related to the ceramic support and the metallic film chemical composition was responsible for the membrane performances.

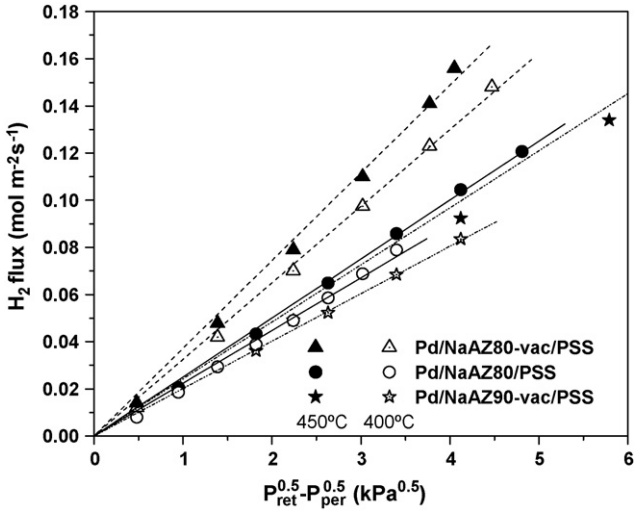

Fig. 8. Sievert's law plots for the three synthesized membranes.

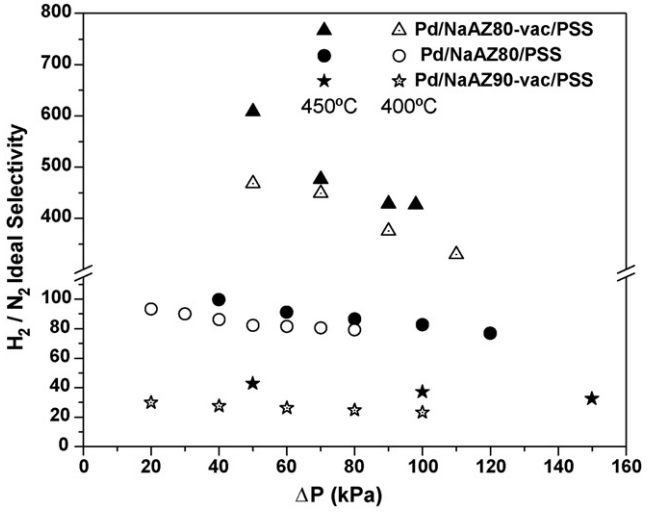

Fig. 9. Effect of the pressure difference upon H_2/N_2 ideal selectivity.

A comparison with some literature results for Pd composite membranes on a stainless steel porous support evaluated under similar conditions, is presented in Table 5. Su et al. [3] employed PSS (separation grade 0.2 μm) to prepare thin palladium membranes, by coating the support with SiO_2 colloidal particles to modify pore size and roughness. The membrane as-synthesized with a thickness of 6 μm, showed a H_2 permeance of 1.9×10^{-3} mol m^{-2} s^{-1} Pa$^{-0.5}$ with a H_2/N_2 ideal selectivity of 450 at 500 °C.

Huang and Dittmeyer [10] aimed at preparing thin defect-free palladium membranes over supports with rough surface. Therefore, they employed PSS modified (310L, pore size of 0.5 μm) with yttria-stabilized zirconia sprayed by atmospheric plasma on top of the support. Their 23 μm thick membrane exhibited a hydrogen permeance equal to 5.2×10^{-4} mol m^{-2} s^{-1} Pa$^{-0.5}$ and a H_2/N_2 ideal selectivity of ~320 at 400 °C.

Palladium membranes on the oxidized surface of a porous stainless steel substrate (316L, 0.2 μm grade support) were synthesized by Rothenberger et al. [27]. They evaluated the palladium membrane performance at high pressure. When the pressure differential during the membrane test was lower than 138 kPa, their best membrane exhibited an infinite selectivity at all pressure conditions. Note that the extremes in the palladium film thickness ranged from about 10 to 50 μm with palladium fingers extending into the pore structure. However, in their case intermetallic diffusion could not be ruled out.

Our Pd/NaAZ80-vac/PSS membrane compares well with the data shown in Table 5.

4. Conclusions

The PSS supports modified with NaA zeolite present N_2 permeance values similar to those reported in the literature, but their thicknesses were significantly lower. The Pd/NaAZ80-vac/PSS membrane with the lowest Pd thickness, shows the best performance with a hydrogen permeance and a H_2/N_2 ideal selectivity of 1.1×10^{-3} mol m^{-2} s^{-1} Pa$^{-0.5}$ and 608, respectively, at 450 °C and 50 kPa. Furthermore, no substrate components were detected in the Pd layer of this membrane. These findings suggest that when vacuum was applied during the zeolite synthesis, an effective intermediate substrate modifier and diffusion barrier was obtained. The H_2/N_2 ideal separation factors and hydrogen permeances of the membranes built with ceramic diffusion barriers are within the same range.

Acknowledgements

The authors wish to acknowledge the financial support received from UNL, CONICET and ANPCyT. They are also grateful to the Japan International Cooperation Agency (JICA) for the donation of the XRD and LRS instruments used in this study and to ANPCyT for Grant PME 8–2003 to finance the purchase of the UHV Multi Analysis System. Thanks are also given to Prof. Elsa Grimaldi for the edition of the English paper and to Fabio Fontanarrosa from CCT CONICET-SANTA FE for the SEM-EDS analyses.

References

[1] Y. Huang, S. Shu, Z. Lu, Y. Fan, Characterization of the adhesion of thin palladium membranes supported on tubular porous ceramics, Thin Solid Films 515 (13) (2007) 5233.
[2] M.E. Ayturk, E.E. Engwall, Y.H. Ma, Microstructure analysis of the intermetallic diffusion-induced alloy phases in composite Pd/Ag/porous stainless steel membranes, Ind. Eng. Chem. Res. 46 (2007) 4295.
[3] C. Su, T. Jin, K. Kuraoka, Y. Matsumura, T. Yazawa, Thin palladium film supported on SiO_2-modified porous stainless steel for a high-hydrogen-flux membrane, Ind. Eng. Chem. Res. 44 (2005) 3053.
[4] Y. Huang, R. Dittmeyer, Preparation and characterization of composite palladium membranes on sinter-metal supports with a ceramic barrier against intermetallic diffusion, J. Membr. Sci. 282 (2006) 296.
[5] J. Tong, Y. Kashima, R. Shirai, H. Suda, Y. Matsumura, Thin defect-free Pd membrane deposited on asymmetric porous stainless steel substrate, Ind. Eng. Chem. Res. 44 (2005) 8025.
[6] Y.H. Ma, B.C. Akis, M.E. Ayturk, F. Guazzone, E.E. Engwall, I.P. Mardilovich, Characterization of intermetallic diffusion barrier and alloy formation for Pd/Cu and Pd/Ag porous stainless steel composite membranes, Ind. Eng. Chem. Res. 43 (2004) 2936.
[7] D. Yepes, L.M. Cornaglia, S. Irusta, E.A. Lombardo, Different oxides used as diffusion barriers in composite hydrogen permeable membranes, J. Membr. Sci. 274 (2006) 92.
[8] F. Guazzone, E.E. Engwall, Y.H. Ma, Effects of surface activity, defects and mass transfer on hydrogen permeance and *n*-value in composite palladium-porous stainless steel membranes, Catal. Today 118 (2006) 24.
[9] D.-W. Lee, Y.-G. Lee, S.-E. Nan, S.-K. Ihm, K.-H. Lee, Study on the variation of morphology and separation behavior of the stainless steel supported membranes at high temperature, J. Membr. Sci. 220 (2003) 137.
[10] Y. Huang, R. Dittmeyer, Preparation of thin palladium membranes on a porous support with rough surface, J. Membr. Sci. 302 (2007) 160.
[11] X. Xu, W. Yang, J. Liu, L. Lin, Synthesis of NaA zeolite membranes from clear solution, Micropor. Mesopor. Mater. 43 (2001) 299.
[12] Ch.J. Gump, V.A. Tuan, R.D. Noble, J.L. Falconer, Aromatic permeation through crystalline molecular sieve membranes, Ind. Eng. Chem. Res. 40 (2001) 565.
[13] S. Miachon, E. Landrivon, M. Aouine, Y. Sun, L. Kumakiri, Y. Li, O. Pachtová Prokopová, N. Guilhaume, A. Giroir-Fendler, H. Mozzanega, J.-A. Dalmon, Nanocomposite MFI-alumina membranes via pore-plugging synthesis preparation and morphological characterisation, J. Membr. Sci. 281 (2006) 228.
[14] A. Huang, W. Yang, J. Liu, Synthesis and pervaporation properties of NaA zeolite membranes prepared with vacuum-assisted method, Sep. Purif. Technol. 56 (2007) 158.
[15] F. Tiscareño-Lechuga, C. Téllez, M. Menéndez, J. Santamaría, A novel device for preparing zeolite-A membranes under a centrifugal force field, J. Membr. Sci. 212 (2003) 135.
[16] P.P. Mardilovich, Y. She, Y.H. Ma, M. Rei, Defect-free palladium membranes on porous stainless-steel support, AIChE J. 44 (1998) 310.
[17] K.L. Yeung, S.C. Christiansen, A. Varma, Palladium composite membranes by electroless plating technique relationships between plating kinetics, film microstructure and membrane performance, J. Membr. Sci. 159 (1999) 107.
[18] X. Xu, Y. Bao, C. Song, W. Yang, J. Liu, L. Lin, Synthesis, characterization and single gas permeation properties of NaA zeolite membrane, J. Membr. Sci. 249 (2005) 51.
[19] C.J. Nuñez, M.V. Utrilla, A. Ureña, Effect of temperature on sintered austeno-ferritic stainless steel microstructure, J. Alloys Compd. 463 (2008) 552.
[20] K. Sato, T. Nakane, A high reproducible fabrication method for industrial production of high flux NaA zeolite membrane, J. Membr. Sci. 301 (2007) 151.
[21] A. Huang, Y.S. Lin, W. Yang, Synthesis and properties of A-type zeolite membranes by secondary growth method with vacuum seeding, J. Membr. Sci. 245 (2004) 41.
[22] J.N. Keuler, L. Lorenzen, R.D. Sanderson, V. Prozesky, W.J. Przybylowicz, Characterization of electroless plated palladium–silver alloy membranes, Thin Solid Films 347 (1999) 91.
[23] M. Brun, A. Berthet, J.C. Bertolini, XPS, AES and Auger parameter of Pd and PdO, J. Electron. Spectrosc. Relat. Phenom. 104 (1999) 55.
[24] F. Morón, M.P. Pina, E. Urriolabeitia, M. Menéndez, J. Santamaría, Preparation and characterization of Pd-zeolite composite membranes for hydrogen separation, Desalination 147 (2002) 425.
[25] W. Mekonnen, B. Arstad, H. Klette, J.C. Walmsley, R. Bredesen, H. Venvik, R. Holmestad, Microstructural characterization of self-supported 1.6 μm Pd/Ag membranes, J. Membr. Sci. 310 (2008) 337.
[26] F. Roa, J.D. Way, R.L. McCormick, S.N. Paglieri, Preparation and characterization of Pd–Cu composite membranes for hydrogen separation, Chem. Eng. J. 93 (2003) 11.
[27] K.S. Rothenberger, A.V. Cugini, B.H. Howard, R.P. Killmeyer, M.V. Ciocco, B.D. Morreale, R.M. Enick, F. Bustamante, I.P. Mardilovich, Y.H. Ma, High pressure hydrogen permeance of porous stainless steel coated with a thin palladium film via electroless plating, J. Membr. Sci. 244 (2004) 55.